

A Photoactivatable AIE Polymer for Light-Controlled Gene Delivery: Concurrent Endo/Lysosomal Escape and DNA Unpacking**

Youyong Yuan, Chong-Jing Zhang, and Bin Liu*

Abstract: Endo/lysosomal escape of gene vectors and the subsequent unpacking of nucleic acids in cytosol are two major challenges for efficient gene delivery. Herein, we report a polymeric gene delivery vector, which consists of a photosensitizer (PS) with aggregation-induced emission (AIE) characteristics and oligoethylenimine (OEI) conjugated via an aminoacrylate (AA) linker that can be cleaved by reactive oxygen species (ROS). In aqueous media, the polymer could self-assemble into bright red fluorescent nanoparticles (NPs), which can efficiently bind to DNA through electrostatic interaction for gene delivery. Upon visible light irradiation, the generated ROS can break the endo/lysosomal membrane and the polymer, resulting in light-controlled endo/lysosomal escape and unpacking of DNA for efficient gene delivery. The smart polymer represents the first successful gene vector to simultaneously address both challenges with a single light excitation process.

Successful gene therapy relies on the development of highly effective and safe vectors.^[1] Nonviral vectors based on electrostatic interactions between synthetic cationic polymers and anionic nucleic acids have been extensively studied.^[2] However, the development of vectors with high transfection efficiency and low cytotoxicity remains challenging. The major barrier is that nonviral vectors generally enter cells through endocytosis and become entrapped in endo/lysosomes, where the nucleic acids tend to be destructed because of the abundance of enzymes there, thus leading to reduced or even no release in cytosol.^[3] Therefore, nucleic acids need to escape from the endo/lysosomes and undergo unpacking for efficient gene delivery.^[4]

Polyethylenimine (PEI), one of the most effective non-viral vectors, can facilitate endo/lysosomal escape by taking

advantage of the “proton sponge effect”.^[5] However, it shows severe cytotoxicity and slow release of nucleic acids. Recently, light-induced endo/lysosomal escape has attracted much attention.^[6] This principle relies on the visible-light-induced generation of reactive oxygen species (ROS) by photosensitizers (PSs), which slightly damages the endo/lysosome membrane. As the light dose used is much lower than that for photodynamic therapy (PDT), this strategy allows the vectors to be liberated from the endo/lysosomes without causing direct cell death or deactivation of nucleic acids.^[7] Since the existing systems are based on coencapsulation of nucleic acids and PSs but no stimuli-triggered DNA release, the gene unpacking from these systems is uncontrollable.

Effective gene unpacking has been realized by reversion of the gene vectors (e.g., high-molecular-weight polycations) to their low-molecular-weight counterparts. The past years have witnessed the development of gene vectors that are responsive to pH, enzymes, reducing agents (e.g. glutathione (GSH)) or light.^[4] The pH- or enzyme-responsive vectors face the challenges of potential DNA release in endo/lysosomes,^[8] which can lead to DNA degradation. Although disulfide conjugated oligoethylenimine (OEI) could achieve endo/lysosomal escape and fast gene release,^[9] the response of the disulfide bond to the high concentration of GSH in cells makes the gene delivery process uncontrollable. Recently, light-responsive systems have attracted much attention for gene delivery.^[10] These gene vectors are largely based on cationic polymers with UV-cleavable linkers, which can realize fast gene unpacking upon UV light irradiation. However, as the UV light used for linker activation^[10] is not compatible with the visible light required for PS excitation, and there has been no report to date that a single polymer vector could be developed for endo/lysosomal escape and concurrent DNA unpacking, not to mention that both processes could be realized in a single irradiation process.

Recently, fluorogens with aggregation-induced emission (AIE) characteristics have attracted increasing attention in biomedical applications.^[11] The AIE fluorogens emit intensively in aggregated states because of the restriction of intramolecular motions.^[11a] The emerging AIE-fluorogen-based PSs with high signal-to-noise ratios and efficient ROS generation in aggregates further offer the opportunity for light-controlled ROS generation and image-guided PDT.^[12] By taking advantage of AIE PSs, we have developed a ROS-responsive polymer for light-controlled gene delivery (Scheme 1). The polymer contains an AIE PS conjugated with OEI (800 Da) via an aminoacrylate (AA) linker that can be cleaved by ROS.^[13] Low-molecular-weight OEIs were selected as the arms because they have lower toxicity than high-molecular-weight PEI, and the OEI conjugates have

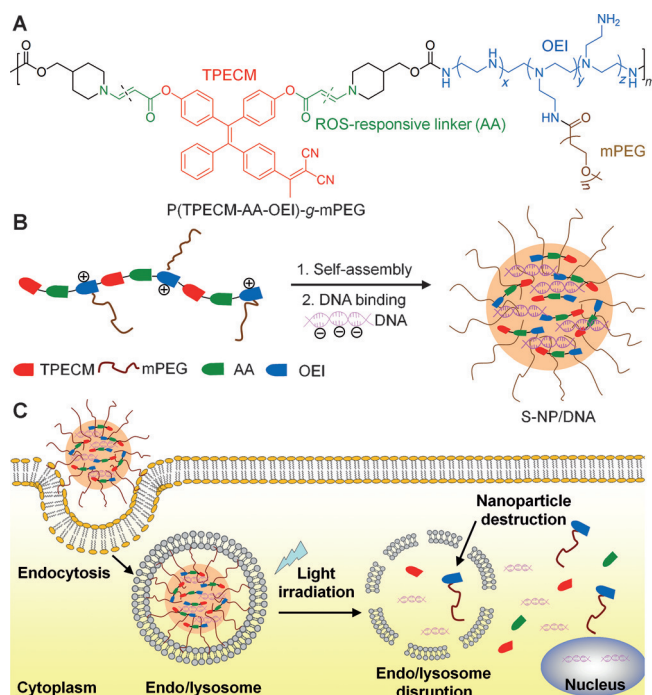
[*] Dr. Y. Yuan,^[†] Dr. C.-J. Zhang,^[†] Prof. B. Liu
Department of Chemical and Biomolecular Engineering
National University of Singapore
4 Engineering Drive, Singapore 117585 (Singapore)
E-mail: cheliub@nus.edu.sg

Prof. B. Liu
Institute of Materials Research and Engineering
Agency for Science, Technology and Research (A*STAR)
3 Research Link, Singapore, 117602 (Singapore)

[†] These authors contributed equally to this work.

[**] We thank the SMART (R279-000-378-592), the Ministry of Education (R279-000-391-112), Singapore NRF Investigatorship (R279-000-444-281) and the Institute of Materials Research and Engineering of Singapore (IMRE/14-8P1110) for financial support. AIE = aggregation-induced emission.

Supporting information for this article is available on the WWW under <http://dx.doi.org/10.1002/anie.201503640>.



shown good DNA-binding ability.^[14] PEG was further grafted to fine-tune the water solubility of the polymer. The polymer can self-assemble into nanoparticles (NPs) in aqueous media with bright red fluorescence for bioimaging. It also can bind to DNA through electrostatic interactions. Upon light irradiation, the generated ROS can facilitate the escape of the vectors from endo/lysosomes by disrupting the membranes. Concurrently, the ROS also breaks the polymer and promotes reversion of the high molecular weight complex back to their low molecular weight counterparts, leading to DNA unpacking. This work represents a promising light-controlled platform for concurrent endo/lysosomal escape and DNA unpacking, which are indispensable steps for efficient gene delivery.

The synthetic routes to the ROS-responsive polymer P(TPECM-AA-OEI)-g-mPEG and the control polymer P(TPECM-OEI)-g-mPEG are shown in Scheme S1 in the Supporting Information. The characterization of the polymer and the intermediates are shown in Figure S1–S5. The amphiphilic P(TPECM-AA-OEI)-g-mPEG can self-assemble in aqueous media to form ROS sensitive NPs (denoted as S-NPs), which were studied by dynamic light scattering (DLS) and transmission electron microscopy (TEM). As shown in Figure 1 A, S-NPs show spherical morphology with a diameter of (134 ± 12) nm. The absorption and emission spectra of

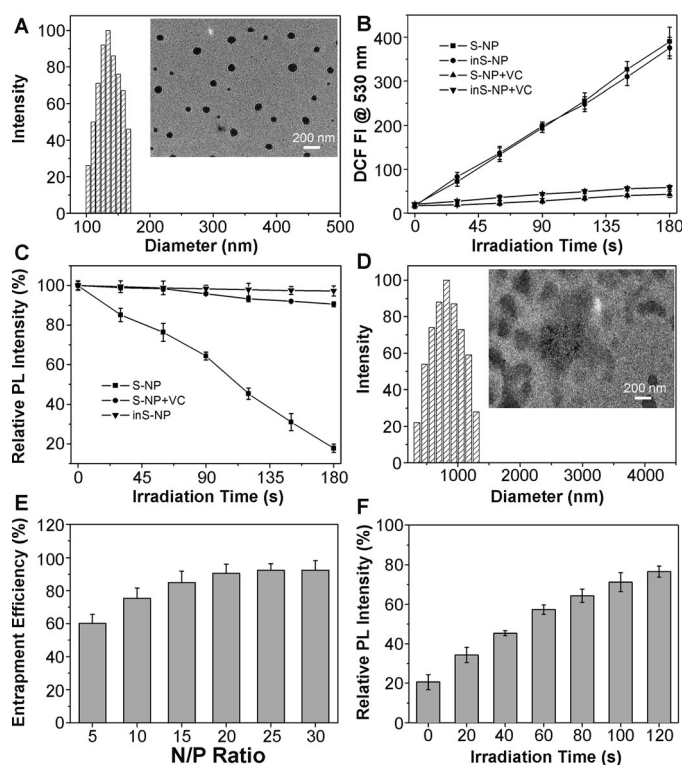


Figure 1. A) Size distribution and TEM image (inset) of S-NPs; B) Time-dependent 2',7'-dichlorofluorescein (DCF) fluorescence intensity (FI) change at 530 nm in S-NPs and inS-NPs with or without VC upon light irradiation; C) Photoluminescence (PL) intensity of Nile Red at 640 nm vs. irradiation time in Nile Red loaded S-NPs, inS-NPs or S-NPs + VC; D) Size distribution and TEM image (inset) of S-NPs after light irradiation. Data represent mean \pm SD ($n=3$). E) DNA entrapment efficiency of S-NPs at different N/P ratios. F) Relative PL intensity changes of YOYO-1 in S-NPs/YOYO-1-DNA at an N/P ratio of 20 upon white light irradiation (50 mW cm^{-2}) for different time periods. Data represent mean \pm SD ($n=3$).

S-NPs are centered at 410 nm and 615 nm, respectively (Figure S6). The control polymer P(TPECM-OEI)-g-mPEG was synthesized without the ROS responsive linker, and the self-assembled NPs are denoted as inS-NPs.

The ROS generation of S-NPs and inS-NPs upon light irradiation was evaluated using dichlorofluorescein diacetate (DCF-DA) as an indicator. DCF-DA is nonfluorescent, but it can be rapidly oxidized by ROS to produce fluorescent dichlorofluorescein (DCF). As shown in Figure 1B, both S-NPs and inS-NPs can quickly and steadily generate ROS upon light irradiation. When vitamin C (VC; a well-known ROS scavenger) was added, the fluorescence increase of DCF was suppressed, which further confirmed the ROS generation by both NPs.

The light-induced destruction of S-NPs was studied using Nile Red as an indicator. Nile Red is a hydrophobic dye that is highly emissive in hydrophobic environments but not in water. Both NPs loaded with Nile Red were irradiated with light and the fluorescence change of Nile Red was studied. As shown in Figure 1C, upon light irradiation, the photoluminescence (PL) intensity of Nile Red in S-NPs decreases steadily to about 20% of its original intensity after 3 min of

irradiation. In contrast, the PL intensity of Nile Red in S-NPs or S-NPs with VC remains constant, thus indicating that the decrease in the Nile Red fluorescence is due to disassembly of the S-NPs (Scheme S2 and Figure S7). This result was also confirmed by a DLS study and TEM images. As shown in the TEM image in Figure 1D, after light irradiation, the diameters of the S-NPs apparently increase and irregular shapes are formed because of the generated hydrophobic AIE residues. In contrast, inS-NPs show negligible changes after light irradiation (Figure S8).

Efficient DNA condensation by S-NPs was confirmed by measuring the particle size and surface charge of S-NPs/DNA complexes. The size of S-NPs/DNA complex decreases while their zeta potential grows with the increased amine to phosphate (N/P) ratios (Figure S9). The DNA entrapment efficiency also increases as a function of the N/P ratio, from $(60 \pm 5)\%$ at $N/P = 5$ to $(92 \pm 6)\%$ at $N/P = 30$ (Figure 1E).

To test whether the light-induced polymer destruction could facilitate DNA unpacking from S-NPs/DNA complexes, YOYO-1 was used as an indicator. YOYO-1 is a DNA intercalating dye that shows strong fluorescence upon binding to DNA. However, when YOYO-1-labeled DNA is condensed with a cationic polymer, it shows dramatically decreased fluorescence because of self-quenching.^[15] As shown in Figure 1F, the fluorescence of YOYO-1 in S-NPs/YOYO-1-DNA intensifies upon light irradiation, thus indicating that the DNA is liberated from the S-NPs. In addition, the irradiation-time-dependent fluorescence change also indicates that the DNA release is light-controllable. In contrast, the fluorescence of YOYO-1 in inS-NPs/YOYO-1-DNA is almost constant upon light irradiation (Figure S10).

The intracellular trafficking profile of S-NPs/DNA complexes was subsequently evaluated by confocal laser scanning microscopy (CLSM). Human cervix carcinoma HeLa cells were incubated with S-NPs/DNA for 4 h and co-stained with endo/lysosome selective marker LysoTracker green DND-26. As shown in Figure 2A3 and 2A4, the red fluorescence from the complex co-localizes well with the green fluorescence from DND-26, indicating that the complexes are entrapped in endo/lysosomes.

We next investigated the ROS-induced endo/lysosomal escaping of S-NPs/DNA and DNA unpacking by CLSM. The ROS generation of S-NPs/DNA in HeLa cells was first confirmed by using DCF-DA as the indicator (Figure S11). When the cells were incubated with S-NPs/YOYO-1-DNA in dark, the red fluorescence of S-NPs and green fluorescence of YOYO-1-labeled DNA are largely overlaid as yellow dots (Figure 2B1). However, upon light irradiation, the cells show notably enhanced separation of green fluorescence from the red (Figure 2B1–4), thus indicating light-induced intracellular DNA release. The unpacked DNA strands spread to the entire cytoplasm, which is a clear indication of their successful escape from the endo/lysosomes. The colocalization ratios of the fluorescence between S-NPs and YOYO-1 decrease from $(83 \pm 3)\%$ to $(24 \pm 5)\%$ after 5 min of light irradiation (Figure 2C). However, this process was prohibited when VC was added, which further confirmed the ROS induced endo/lysosomal escape and light-controlled DNA unpacking. When the cells were pretreated with the endo/lysosomal disrupting

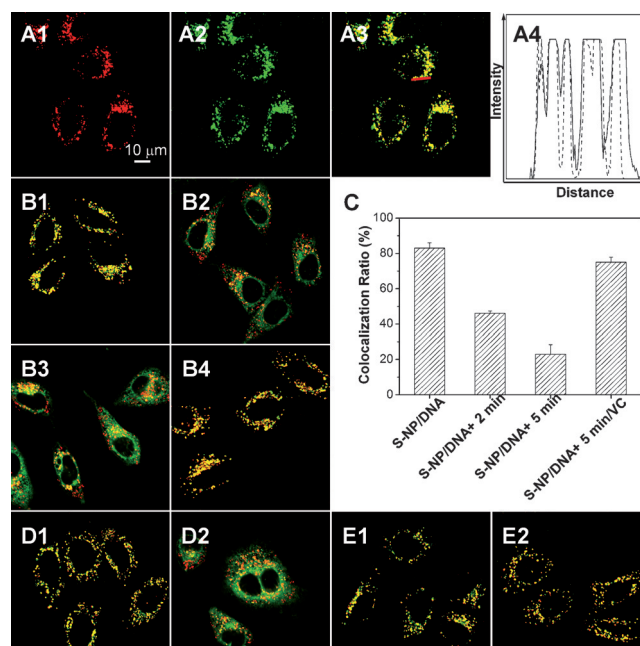


Figure 2. A) CLSM images of HeLa cells stained with S-NPs/DNA (A1, E_x : 405 nm, E_m : > 560 nm) and LysoTracker green (A2, E_x : 488 nm, E_m : 505–525 nm); overlay of the images A1 and A2 (A3); intensity profiles of region of interest (A4; red line in image A3; solid line = lyso tracker, dashed line = S-NP/DNA). B) CLSM images of HeLa cells incubated with S-NPs/YOYO-1-DNA complexes in the dark (B1), with light irradiation for 2 min (B2), 5 min (B3), and 5 min in the presence of VC (B4). Green: YOYO-1 fluorescence (E_x : 488 nm; E_m : 505–525 nm); Red: S-NPs fluorescence (E_x : 405 nm; E_m : > 560 nm). Yellow: colocalization of red and green pixels. C) Changes in colocalization ratios between the fluorescence of YOYO-1 and S-NPs after different treatment. D, E) CLSM images of HeLa cells after incubation with D) S-NPs/YOYO-1-DNA pretreated with chloroquine (CQ), E) inS-NPs/YOYO-1-DNA in the dark (D1, E1) or after 5 min light irradiation (D2, E2). Scale bar for all images is 10 μ m.

agent chloroquine (CQ)^[16] in the absence of light treatment, limited DNA release was observed (Figure 2D). However, the yellow dots were dispersed all over the cells, thus indicating that the YOYO-1-labeled DNA strands had already escaped from the endo/lysosomes but still condensed with S-NPs. Further treatment with 5 min of light irradiation, the green fluorescence was spread all over the cytoplasm (Figure 2D2), thus indicating that DNA could be released after polymer breakdown. When the cells were treated with inS-NPs/YOYO-1-DNA, the DNA strands could not be released from the vectors (Figure 2E1,E2).

The ROS-induced endo/lysosomal damage was further confirmed using acridine orange (AO) as an indicator. AO emits red fluorescence in acidic organelle such as endo/lysosomes and emits green fluorescence in cytoplasm and nuclei. As shown in Figure 3, without ROS, the HeLa cells show both red and green fluorescence, indicating that the endo/lysosomes are not damaged. However, the red fluorescence was remarkably reduced when the cells were exposed to light irradiation or treated with CQ, thus indicating that the endo/lysosomes were destroyed.

As gene expression takes place in cell nuclei, effective accumulation of DNA in nuclei is essential for gene deliv-

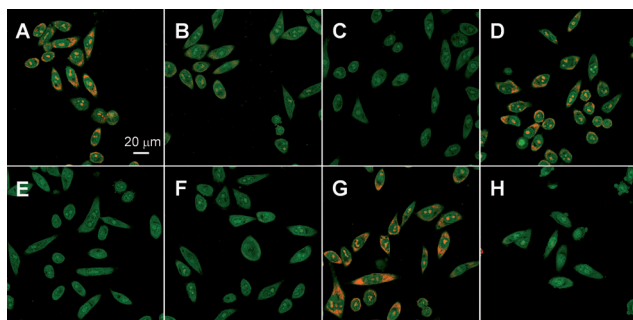


Figure 3. Observation of endo/lysosomal disruption of HeLa cells induced by ROS or CQ using acridine orange (AO, 5 μM) as the indicator. The cells were treated with S-NPs/DNA A) in the dark; with light irradiation for B) 2 min; C) 5 min; D) 5 min in the presence of VC; E) S-NPs/DNA in the presence of CQ in the dark; F) S-NPs/DNA in the presence of CQ with 5 min light irradiation; G) inS-NPs/DNA in the dark; H) inS-NPs/DNA with 5 min light irradiation. The power density was 50 mWcm^{-2} . E_x : 488 nm; E_m : 505–525 nm (green); 610–640 nm (red). Scale bar for all images is 20 μm .

ery.^[2] After light irradiation, the cells were further incubated in fresh medium for 4 h and the cell nuclei were live-stained with DRAQ5. As shown in Figure S12, the red fluorescence of DRAQ5 and green fluorescence of YOYO-1 were only overlapped when the cells were incubated with S-NPs/YOYO-1-DNA and under light irradiation. This is evidenced by the yellow color in the overlay image, which indicates that the released DNA is accumulated in nuclei.

The transfection efficiency of HeLa cells was studied by flow cytometry using plasmid encoding enhanced green fluorescent protein (EGFP). As shown in Figure 4A, the GFP transfection efficiency in HeLa cells incubated with S-NPs/DNA with light irradiation is $(68 \pm 6)\%$, which is significantly higher than that of the cells incubated with S-NPs/DNA in the dark $((31 \pm 2)\%)$ or in the presence of VC $((35 \pm 3)\%)$. The S-NPs/DNA treated with CQ show slightly higher transfection efficiency $((39 \pm 5)\%)$ than that in the dark, which should be due to the enhanced endo/lysosomal escape. After light irradiation, the higher transfection efficiency $((71 \pm 4)\%)$ should be due to the optimized DNA

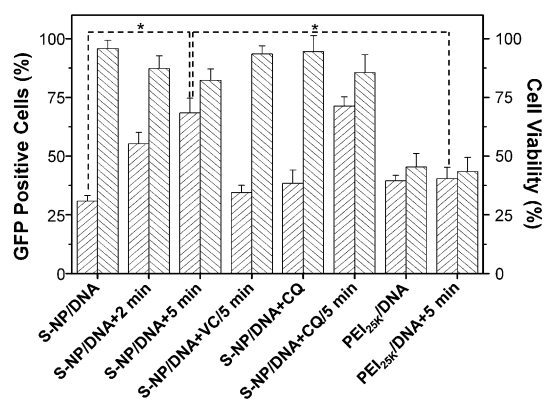


Figure 4. Transfection efficiencies (left column) and cell viabilities (right column) of HeLa cells after different treatments. * indicates $p < 0.05$.

release after polymer breakdown. These results demonstrate that endo/lysosomal escape and DNA unpacking are indispensable steps for efficient gene delivery. In addition, S-NPs/DNA also showed significantly higher transfection efficiency upon light irradiation than the commercially available transfection agent PEI_{25k} (Figure S13), which should be due to the slow DNA release from PEI_{25k}.^[17] The same trend is also observed for several other cell lines, which include human hepatocellular liver carcinoma HepG2 cells; human lung adenocarcinoma epithelial A549 cells; human embryonic kidney HEK293 cells and murine fibroblast NIH 3T3 cells (Figure S14), thus confirming the generality of the method. In addition to higher gene-transfection efficiency, S-NPs/DNA also showed lower cytotoxicity than PEI_{25k}/DNA under light irradiation, thus indicating the lower toxicity of the low-molecular-weight OEI after photoinduced polymer breakdown (Figure S15).

In summary, we developed a novel photoactive polymer that is composed of an AIE photosensitizer and OEI conjugated via a ROS-responsive linker for light-controlled gene delivery. Upon light irradiation, the polymer vector can concurrently induce endo/lysosomal escape and DNA unpacking, which is able to efficiently deliver DNA to the cytosol of cells with low cytotoxicity. In all the tested cell lines, the ROS-responsive polymer showed on average over 50% increase of transfection efficiency as compared to that with the commercial PEI_{25k}. The single light irradiation has successfully triggered multiple responses to overcome different barriers in nonviral gene delivery. By substituting the nucleic acids with therapeutic DNA or siRNA, the vectors developed in this work offer a simple yet effective strategy for efficient gene therapy. The same design strategy can also be applied for general cytosolic drug delivery.

Keywords: aggregation-induced emission · endo/lysosomes · gene delivery · polymers · reactive oxygen species

How to cite: *Angew. Chem. Int. Ed.* **2015**, 54, 11419–11423
Angew. Chem. **2015**, 127, 11581–11585

- [1] M. A. Kay, *Nat. Rev. Genet.* **2011**, 12, 316.
- [2] X. Guo, L. Huang, *Acc. Chem. Res.* **2012**, 45, 971.
- [3] a) M. A. Mintzer, E. E. Simanek, *Chem. Rev.* **2009**, 109, 259; b) J. Nguyen, F. C. Szoka, *Acc. Chem. Res.* **2012**, 45, 1153.
- [4] a) D. V. Schaffer, N. A. Fidelman, N. Dan, D. A. Lauffenburger, *Biotechnol. Bioeng.* **2000**, 67, 598; b) H. Y. Kuchelmeister, A. Gutschmidt, S. Tillmann, S. Knauerb, C. Schmuck, *Chem. Sci.* **2012**, 3, 996; c) K. Luo, B. He, Y. Wu, Y. Q. Shen, Z. W. Gu, *Biotechnol. Adv.* **2014**, 32, 818.
- [5] O. Boussif, F. Lezoualch, M. A. Zanta, M. D. Mergny, D. Scherman, B. Demeneix, J. P. Behr, *Proc. Natl. Acad. Sci. USA* **1995**, 92, 7297.
- [6] T. Nomoto, S. Fukushima, M. Kumagai, K. Machitani, A. Arnida, Y. Matsumoto, M. Oba, K. Miyata, K. Osada, N. Nishiyama, K. Kataoka, *Nat. Commun.* **2014**, 5, 3545.
- [7] a) A. Högset, B. O. Engesæter, L. Prasmickaite, K. Berg, O. Fodstad, G. M. Mælandsmo, *Cancer Gene Ther.* **2002**, 9, 365; b) X. Wang, K. Liu, G. B. Yang, L. Cheng, L. He, Y. M. Liu, Y. G. Li, L. Guo, Z. Liu, *Nanoscale* **2014**, 6, 9198; c) K. Han, L. Qi, H. Jia, S. Wang, W. Yin, W. Chen, S. Cheng, X. Zhang, *Adv. Funct. Mater.* **2015**, 25, 1248.
- [8] M. S. Shim, Y. J. Kwon, *Adv. Drug Delivery Rev.* **2012**, 64, 1046.

- [9] a) M. Ou, R. Z. Xu, S. H. Kim, D. A. Bull, S. W. Kim, *Biomaterials* **2009**, *30*, 5804; b) F. H. Meng, W. E. Hennink, Z. Zhong, *Biomaterials* **2009**, *30*, 2180; c) J. Li, C. Zheng, S. Cansiz, C. C. Wu, J. H. Xu, C. Cui, Y. Liu, W. J. Hou, Y. Y. Wang, L. Q. Zhang, T. Teng, H. H. Yang, W. H. Tan, *J. Am. Chem. Soc.* **2015**, *137*, 1412.
- [10] a) M. A. Kostianen, D. K. Smith, O. Ikkala, *Angew. Chem. Int. Ed.* **2007**, *46*, 7600; *Angew. Chem.* **2007**, *119*, 7744; b) L. C. Yin, H. Y. Tang, K. H. Kim, N. Zheng, Z. Y. Song, N. P. Gabrielson, H. Lu, J. J. Cheng, *Angew. Chem. Int. Ed.* **2013**, *52*, 9182; *Angew. Chem.* **2013**, *125*, 9352.
- [11] a) R. T. Kwok, C. W. Leung, J. W. Lam, B. Z. Tang, *Chem. Soc. Rev.* **2015**, DOI: 10.1039/C4CS00325J; b) D. Ding, K. Li, B. Liu, B. Z. Tang, *Acc. Chem. Res.* **2013**, *46*, 2441; c) X. Zhang, X. Zhang, L. Tao, Z. Chi, J. Xu, Y. Wei, *J. Mater. Chem. B* **2014**, *2*, 4398; d) Q. L. Hu, M. Gao, G. X. Feng, B. Liu, *Angew. Chem. Int. Ed.* **2014**, *53*, 14225–14229; *Angew. Chem.* **2014**, *126*, 14449–14453; e) X. R. Wang, J. M. Hu, G. Y. Zhang, S. Y. Liu, *J. Am. Chem. Soc.* **2014**, *136*, 9890.
- [12] a) Y. Yuan, C. J. Zhang, M. Gao, R. Zhang, B. Z. Tang, B. Liu, *Angew. Chem. Int. Ed.* **2015**, *54*, 1780; *Angew. Chem.* **2015**, *127*, 1800; b) F. Hu, Y. Y. Huang, G. X. Zhang, R. Zhao, H. Yang, D. Q. Zhang, *Anal. Chem.* **2014**, *86*, 7987; c) Y. Y. Yuan, G. X. Feng, W. Qin, B. Z. Tang, B. Liu, *Chem. Commun.* **2014**, *50*, 8757–8760.
- [13] a) S. H. Lee, M. K. Gupta, J. B. Bang, H. Bae, H. J. Sung, *Adv. Healthcare Mater.* **2013**, *2*, 908; b) B. Moses, Y. You, *Med. Chem.* **2013**, *3*, 192.
- [14] D. Fischer, T. Bieber, Y. X. Li, H. P. Elsasser, T. Kissel, *Pharm. Res.* **1999**, *16*, 1273.
- [15] G. Krishnamoorthy, G. Duportail, Y. Mely, *Biochemistry* **2002**, *41*, 15277.
- [16] J. S. Wadia, R. V. Stan, S. F. Dowdy, *Nat. Med.* **2004**, *10*, 310.
- [17] M. Bertschinger, G. Backliwal, A. Schertenleib, M. Jordan, D. L. Hacker, F. M. Wurm, *J. Controlled Release* **2006**, *116*, 96.

Received: April 21, 2015

Published online: June 19, 2015